Dyes and Pigments 95 (2012) 443–449

Contents lists available at SciVerse ScienceDirect

Dyes and Pigments

journal homepage: www.elsevier.com/locate/dyepig

Preparation and photocatalytic property of hexagonal cylinder-like bipods ZnO microcrystal photocatalyst

Yumin Liu*, Hua Lv, Shuangqing Li, Xinyan Xing, Guoxi Xi

College of Chemistry and Environmental Science, Henan Normal University, Xinxiang 453007, Henan, PR China

ARTICLE INFO

Article history:
Received 25 February 2011
Received in revised form
29 April 2012
Accepted 10 May 2012
Available online 29 June 2012

Keywords:
ZnO
Hydrothermal microemulsion method
Photocatalytic
Reactive Brilliant Red K-2BP
Intermediate compounds
Degradation mechanism

ABSTRACT

Single crystalline ZnO with hexagonal cylinder-like bipods morphologies were successfully synthesized via a cationic surfactant-assisted hydrothermal microemulsion route. The structure, morphologies and properties of the as-prepared samples were determined using X-ray diffraction, scanning electron microscopy, photoluminescence spectrum and Ultraviolet and Visible absorption spectroscopy. The photocatalytic activities of the obtained products were evaluated by the degradation of Reactive Brilliant Red K-2BP in aqueous solution under a variety of conditions. Under the optimum condition, approximately 99.5% decolorization efficiency within 45 min and 65.3% TOC removal efficiency within 3 h were achieved, which were higher than that by the commercial ZnO. Moreover, the degradation products were analyzed by a gas chromatography coupled with mass spectrometry system and the probable pathways for the formation of the intermediates were proposed. The photocatalytic results indicated that the as-prepared ZnO showed good photocatalytic activity and it could be considered as a promising photocatalyst for dyes wastewater treatment.

© 2012 Elsevier Ltd. All rights reserved.

1. Introduction

Large amounts of colored dye wastewaters released into environment mainly by dyestuff and textile industry lead to severe surface water and groundwater contamination [1,2]. Conventional methods such as physical methods, chemical methods or their combinations are used for decolorization of these dyes [3]. Nevertheless, these methods are usually non-destructive, inefficient, costly and result in secondary pollution. Thus, it is necessary to develop treatment methods that are more effective in eliminating dyes from wastewaters.

Advanced oxidation processes (AOPs) have been developed to meet the increasing need of an effective wastewater treatment, which are characterized by the generation of highly oxidative hydroxyl radicals in the homogeneous or heterogeneous phase [4]. Among AOPs, cheaply available nontoxic semiconductors (TiO_2, ZnO) are the most extensively used photocatalysts due to their high photocatalytic activity. It is well known that TiO_2 is universally considered as the most active photocatalyst, while ZnO is found to be a suitable alternative to TiO_2 because its photodegradation mechanism has been proven to be similar to that of TiO_2 [5]. The biggest advantage of ZnO compared with TiO_2 is that it absorbs a larger fraction of the UV spectrum and more light quanta [6]. In addition, it has been reported that ZnO shows better activity than that of TiO_2 in the photodegradation of some dyes in aqueous solutions [7,8].

As is well known, the size and morphology of semiconductors have great influences on their properties. Up to date, different morphologies and sizes of ZnO have been successfully synthesized, including nanowires [9], nanowhiskers [10], tubes [11], star-like [12], tetrapod-like [13] and flower-like [14], etc. However, despite great progress in this field, the shape-controlled synthesis of ZnO materials still remains a remarkable challenge. Various approaches have been employed to synthesize ZnO with unique microstructures, such as thermal decomposition method [15], homogeneous precipitation [16], hydrothermal method [17], sol–gel processing [18], microwave method [19], hydrothermal microemulsion [20] and microemulsion method [21], etc. Among them, hydrothermal microemulsion method is a promising method for synthesizing ideal ZnO materials with special morphology. The main advantage of this method is low reaction temperature and short processing time that prevent agglomeration in the formed particles.

Recently, studies on synthesis of ZnO composed of hexagonal microstructures have been reported [22–24]. For example, Sun and Qiu have reported synthesis of single-crystalline ZnO microtubes with hexagonal shape by gas method [22]. Bitenc et al. have reported on the fabrication of hexagonal bipods ZnO by a facile-

* Corresponding author. Tel.: +86 373 3326335; fax: +86 373 3326336.
E-mail address: ymliu2007@163.com (Y. Liu).

0143-7208/$ – see front matter © 2012 Elsevier Ltd. All rights reserved.
http://dx.doi.org/10.1016/j.dyepig.2012.05.027

template-free method in a mixture of water and ethylene glycol [23]. However, few efforts have been made to synthesize ZnO with hexagonal cylinder-like bipods morphology by hydrothermal microemulsion route to the best of our knowledge. In this paper, ZnO with hexagonal cylinder-like bipods morphology was successfully synthesized via a cationic surfactant-assisted hydrothermal microemulsion route. The structure, morphologies and properties of the as-prepared products were characterized by X-ray diffraction (XRD), scanning electron microscopy (SEM), transmission electron microscopy (TEM), photoluminescence (PL) spectrum and Ultraviolet and Visible absorption spectroscopy (UV–Vis). The photocatalytic activities of the prepared ZnO microcrystal photocatalyst were evaluated by the degradation of Reactive Brilliant Red K-2BP and a possible degradation pathway of the reactive dye was proposed.

2. Materials and methods

2.1. Materials

The dye of Reactive Brilliant Red K-2BP (purity $\geq$ 98%) was purchased from the Eighth Dye Chemical Factory of Shanghai (Shanghai, China) and used directly without further purification. All other chemicals were of reagent grade and used as received.

2.2. Preparation of hexagonal cylinder-like bipods ZnO

In a typical experimental procedure, two identical solutions were separately prepared by dissolving CTAB (2 g) in 20 ml of cyclohexane and 4 ml of n-butanol. Then, 2 ml of 0.5 M zinc acetate dihydrate and 2 ml of 0.25 M methenamine aqueous solutions were added to the two solutions, respectively. After vigorous stirring at room temperature for 30 min, the two optically transparent microemulsion solutions were mixed and stirred for another 30 min. The resulting microemulsion was transferred into a Teflon-lined stainless-steel autoclave and heated at 140 °C for 14 h, followed by cooling to room temperature naturally. White products were separated by centrifugation and washed with deionized water and absolute ethanol several times. Then, the obtained products were dried in a vacuum at 50 °C for 12 h.

2.3. Characterization of hexagonal cylinder-like bipods ZnO

The crystal structure of the synthesized ZnO was determined by XRD (Bruker D8 Advance, Germany) using graphite monochromatic copper radiation (Cu Kα) in the 2θ range of 20–80°. The crystal morphology of ZnO was observed by SEM (JEOL JSM-63901, Japan) and TEM (JEOL JEM-2100, Japan). The specific surface area of the ZnO powder was determined, in terms of the N_2 adsorption on the powder, using the standard Brunauer–Emmett–Teller (BET) procedure. The measurement was performed using a volumetric adsorption apparatus (NOVA Surface Area Analyzer Station A, USA). The optical absorption spectra of ZnO were recorded by UV–Vis spectrophotometer (Lambda 17, PerkinElmer, USA). Prior to UV–Vis analysis the ZnO samples were ultrasonically dispersed in deionized water at room temperature. The room temperature photoluminescence (PL) spectra of ZnO microcrystal were measured by using a Fluorescence Spectrophotometer (FP-6500, Japan) equipped with a Xenon lamp at an excitation wavelength of 325 nm.

2.4. Photocatalytic experiments

The photocatalytic activities of the hexagonal cylinder-like bipods ZnO were evaluated by photocatalytic degradation of Reactive Brilliant Red K-2BP solution. All experiments were carried out in a photoreaction apparatus as reported in our previous study [25]. A 300 W high-pressure mercury lamp with the strongest emission at 365 nm was used as light source (Shanghai Jiguang Company, China). The temperature of the reactions was controlled at room temperature by circulating water. The pH value of the solution was controlled by adding 0.5 M HCl or NaOH solution. In all experiments, 500 ml of the dye solution containing appropriate quantity of ZnO suspensions was used. The suspension was sonicated for 10 min and stirred for 30 min in the dark in order to reach the adsorption–desorption equilibrium. At specific time intervals, 5 ml of the sample was withdrawn and centrifuged to separate the catalyst before analysis.

For the determination of the dye concentration, UV–Vis spectrophotometer (Model T60, Beijing Purkinje General Instrument Company, China) was used at λ_{max} of 537 nm. The total organic carbon (TOC) of the dye before and after decolorization was also measured by using a TOC analyzer (Apollo 9000, Terkmar Dohrmann, USA).

The degradation products were identified using a gas chromatography coupled with mass spectrometry (GC/MS) system. The samples collected at different time intervals during the degradation process were acidified and extracted with dichloromethane. The extracts were dehydrated using anhydrous sodium sulfate. Afterward, the dehydrated solution was concentrated to 1 ml. The GC system (TRACE GC, Thermo Fishier) was equipped with a TR-35MS capillary chromatographic column (30 m $\times$ 0.25 mm, 0.25 μm) and coupled to a MS system (DSQII, Finnigan). The injection was conducted on a splitless mode, and the injector temperature was 300 °C with helium served as the carrier gas at the flow rate of 1.0 ml min^{-1}. The extracted samples were chromatographed under the following temperature gradient: the initial column temperature was held constant at 50 °C for 5 min, increased at 10 °C min^{-1} to 100 °C and kept constant for 2 min, then ramped at 8 °C min^{-1} to 250 °C and maintained constant for 5 min, further increased at 20 °C min^{-1} to 280 °C and retained constant for 5 min, and finally raised at 25 °C min^{-1} to 300 °C and stayed constant for 5 min.

3. Results and discussion

3.1. Characterization of the ZnO microcrystal photocatalyst

A typical XRD pattern of the synthesized ZnO is shown in Fig. 1. All the diffraction peaks in Fig. 1 can be well indexed to the hexagonal wurtzite ZnO (JCPDS card No. 65-3411). The results indicate that the products consist of pure phase and no characteristic peaks can be found from other impurities. The sharp and strong diffraction peaks reveal that the as-synthesized products are of high purity and good crystallinity.

Fig. 2 shows the typical SEM and TEM images of the prepared and commercial ZnO. It can be observed that the synthesized ZnO exhibits an obviously different microstructure compared to the commercial ZnO. As shown in Fig. 2a and b, hexagonal cylinder-like bipods ZnO about 1 μm in diameter and 2.5 μm in length are observed and a bipod structure can be clearly seen in the middle of the hexagonal cylinder. A typical TEM image of the single hexagonal cylinder-like bipod is shown in Fig. 2d. It is clear that the morphology of samples is in accordance with the results of the SEM. The corresponding selected area electron diffraction (SAED) pattern of the synthesized ZnO demonstrates that the grown products are single-crystalline and grown along the *c*-axis direction in preference. On the contrary, various microstructures were observed from the SEM image of the commercial ZnO (Fig. 2c). Although the commercial ZnO exhibits a smaller particle size than that of the prepared ZnO, it also can be seen from Fig. 2c that the

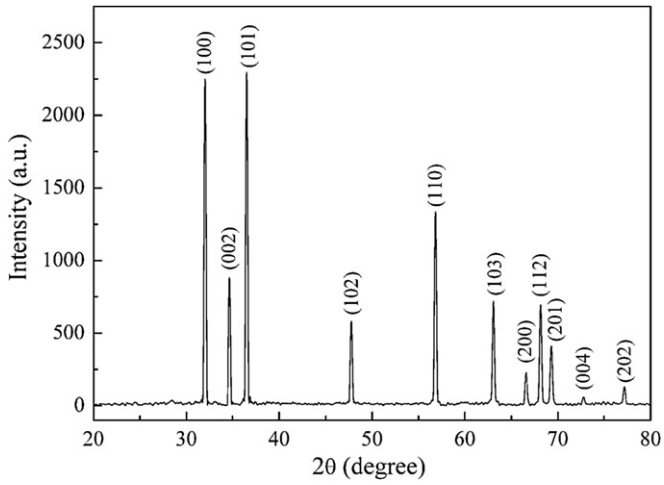

Fig. 1. XRD pattern of the synthesized ZnO.

commercial ZnO particles are easy to agglomerate with each other, which can result in the decreasing light utilization rate and lower photocatalytic activity. The specific surface area of the synthesized and commercial ZnO, measured using the BET method, were 8.60 and 2.47 m^2/g, respectively, which means that the hexagonal shape and bipod structure can increase the surface area of the prepared ZnO and consequently enhance its light absorption.

Previous report has been demonstrated that dumbbell-like ZnO twinned crystals can be formed by the hydrothermal process using KBr or $NaNO_2$ as the mineralizer [26]. In such a hydrothermal process, K^+ or Na^+ may be taken as the bond bridge between the growth units to form a crystal nucleus of the dumbbell-like twinning crystal. In our case, the growth units of $[Zn(OH)_4]^{2-}$ can be bonded by the CTAB to form the nucleus of hexagonal cylinder-like bipod crystal. To decrease the surface energy, the growth of the individual bipod crystallite took place along the polar *c*-axis by means of the incorporation of growth units on the growth interfaces (0001) and thus hexagonal cylinder-like bipods ZnO crystals were formed ultimately.

The absorption of UV–Vis light is an important factor for the evaluation of photocatalyst property. Fig. 3 shows the UV–Vis absorption spectra of the prepared and commercial ZnO. The prepared ZnO microcrystal photocatalyst has a broad absorption band from ultraviolet to visible region and the maximum absorption peak is found at 375 nm. On the contrary, the commercial ZnO shows narrower and weaker absorption in this region. The broad band-edge absorption of the synthesized ZnO may be attributed to its bipods microstructure and further investigation is needed for detailed explanation.

The room temperature photoluminescence (PL) spectra of the prepared and commercial ZnO were recorded as shown in Fig. 4. For the commercial ZnO, it has an UV emission band at about 383 nm and several blue and green emission peaks at 420–550 nm. The UV emission peak at 383 nm is due to the recombination of photogenerated electrons and holes, while the blue and green emission peaks are possibly associated with oxygen vacancies [27]. For the as-prepared ZnO, only a very strong peak at 386 nm corresponding to the near band-edge emission is observed, which means that the synthesized ZnO are highly crystalline with no oxygen vacancies. It is commonly accepted that high-quality ZnO crystals only emit UV light. Therefore, it is reasonably believed that the synthesized ZnO crystals with hexagonal cylinder-like bipods morphology are of good quality and may have wide application in the photocatalytic field.

3.2. Degradation

3.2.1. Spectral changes of Reactive Brilliant Red K-2BP during decolorization process

Fig. 5 shows the UV–Vis spectrum obtained for the Reactive Brilliant Red K-2BP solution during the decolorization process

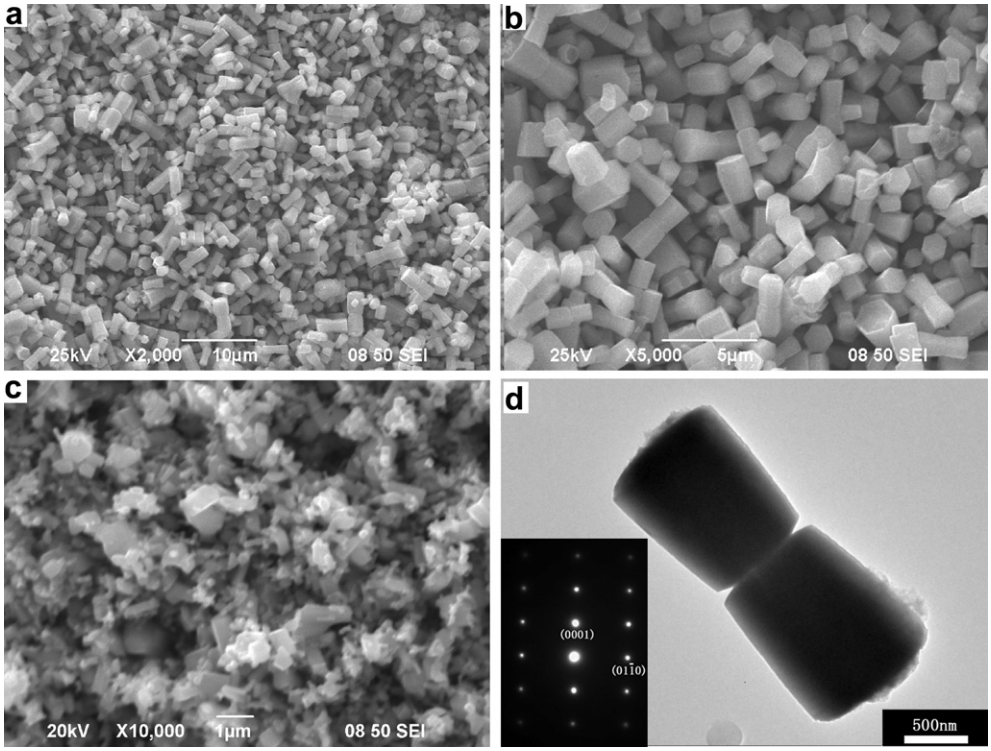

Fig. 2. SEM images of the synthesized ZnO (a and b) and commercial ZnO (c). (d) Low-magnification TEM image of the synthesized ZnO. Inset in part d is the SAED pattern of the synthesized ZnO.

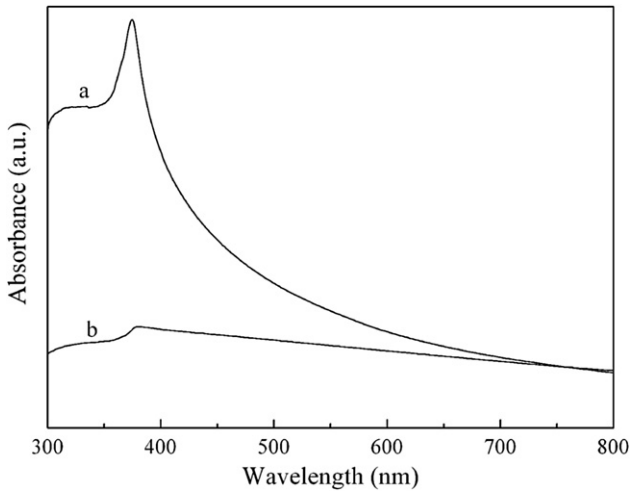

Fig. 3. UV–Vis absorption spectra of the synthesized ZnO (a) and commercial ZnO (b).

taken along time in a typical experiment. Regarding the dye spectrum, it is characterized by three bands in the ultraviolet region located at 247, 288 and 378 nm and by one band in the visible region, with a maximum located at 537 nm. The absorbance peaks in the UV region can be assigned to the benzene, triazine and naphthalene rings [28], whereas the band observed in the visible region can be attributed to chromophore-containing azo linkage of Reactive Brilliant Red K-2BP [29]. By comparing the original spectrum ($t = 0$ min) with that achieved within 45 min of decolorization, it is evident that the treated dye sample is almost colorless and doesn't show significant absorbance in the visible region, indicating that color removal is practically complete. The disappearance of the absorbance peak at 537 nm reflects, unequivocally, the breakdown in the chromophoric group. However, the spectrum in the ultraviolet region shows that the dye is not completely mineralized, even though the absorption intensity is reduced within the ultraviolet range. The slower decrease of the intensities of the bands in the ultraviolet region, with respect to that of the azo bond, can be attributed to the formation of intermediates, resulting from the decolorization of the azo dye, which still contain benzoic-and naphthalene-type rings [30].

3.2.2. Effect of catalyst dosage

The influence of catalyst dosage on the decolorization efficiency against time is illustrated in Fig. 6. The decolorization efficiency

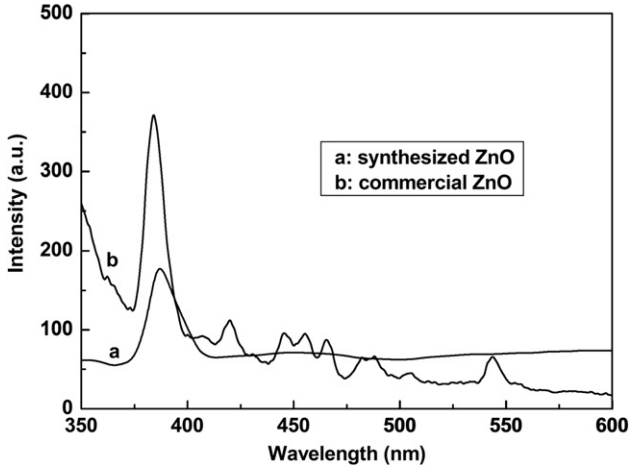

Fig. 4. PL spectra of the ZnO samples at room temperature.

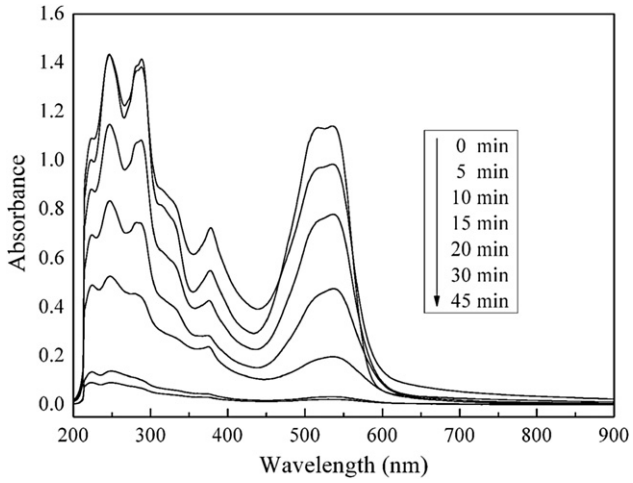

Fig. 5. Variation of UV–Vis absorbance spectra of Reactive Brilliant Red K-2BP with different reaction time under UV light irradiation in the presence of the synthesized ZnO. Experimental conditions: [ZnO] = 0.5 g/l, pH = 6.0, and [dye] = 50 mg/l.

increases sharply from 11.5 to 99.5% after 45 min irradiation when the concentration of the catalyst increases from 0 to 0.5 g/l. Higher reaction rates at higher amount of catalyst loading may be explained in terms of the complete utilization of incident photons striking on the catalyst surface and/or availability of active sites at the surface [31]. Nevertheless, it should be pointed out that the decolorization efficiency decreases to 97.9% with further increasing the ZnO dosage to 0.7 g/l. These observations can be rationalized in terms of availability of active sites on ZnO surface and the penetration of photo activating light into the suspension. Firstly, high catalyst concentration may lead to the aggregation of ZnO particles, which consequently causes a decrease in the number of surface active sites and reduces the catalytic activity. Secondly, high catalyst concentration can increase opacity of the suspension and light scattering, and thus decreases the passage of irradiation through the sample [32]. On the basis of these results, 0.5 g/l is selected as the optimum dosage of ZnO for the subsequent experiments.

3.2.3. Effect of initial pH

The influence of pH on the decolorization of Reactive Brilliant Red K-2BP was studied with pH ranging from 4.0 to 10.0. As it is presented in Fig. 7, the color removal increases significantly from

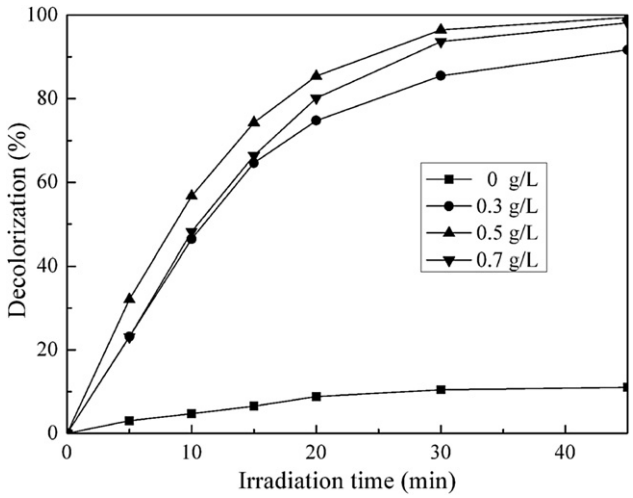

Fig. 6. Effect of catalyst dosage on the photocatalytic degradation of Reactive Brilliant Red K-2BP. Experimental conditions: pH = 6.0 and [dye] = 50 mg/l.

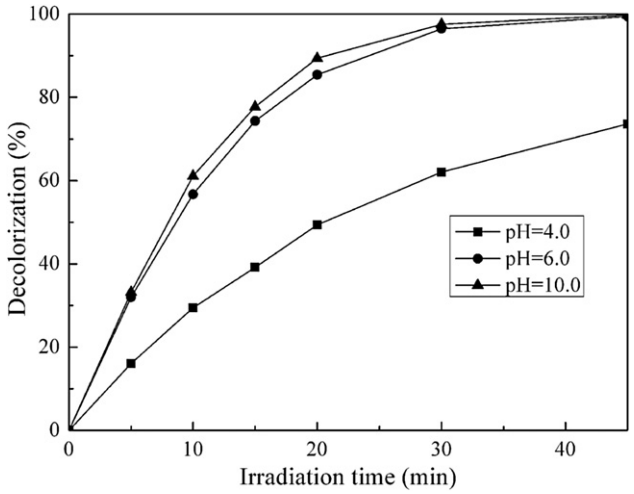

Fig. 7. Effect of initial pH on the photocatalytic degradation of Reactive Brilliant Red K-2BP. Experimental conditions: [dye] = 50 mg/l and [ZnO] = 0.5 g/l.

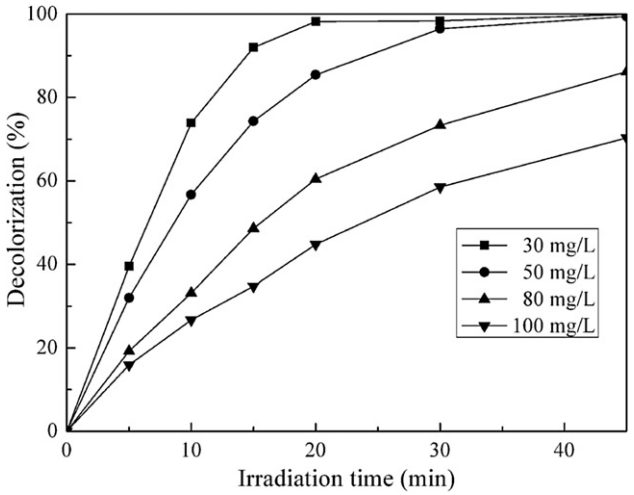

Fig. 8. Effect of initial dye concentration on the photocatalytic degradation of Reactive Brilliant Red K-2BP. Experimental conditions: pH = 6.0 and [ZnO] = 0.5 g/l.

73.7% at a pH of 4.0 to 99.5% at a pH of 6.0, and then increases slightly with the increase of pH to 10.0. The point worthy to mention is that the results indicate alkaline conditions can promote photocatalytic performance. The possible explanation is that ZnO is a poor photocatalyst in the oxidative degradation of Reactive Brilliant Red K-2BP at pH 4.0, because it corrodes in aqueous acidic media [33]. In alkaline medium, excess of hydroxyl anions typically act as scavenger of holes on the surface of ZnO and become hydroxyl radicals with strong oxidation ability after they lose electrons. Consequently, a higher concentration of •OH species is formed, and the decolorization efficiency is enhanced [34]. Because the difference between the decolorization efficiency in the basic solution (about 10.0) and in its natural solution (about 6.0) is very small, the pH value of 6.0 is chosen as a moderate and optimum pH value and the experiments is followed under this pH value.

3.2.4. Effect of initial dye concentration

It is important from an application point of view to study the dependence of dye concentration on the photocatalytic reaction rate. As shown in Fig. 8, the effect of initial dye concentration was investigated by varying the initial concentration from 30 to 100 mg/l. The decolorization efficiency decreases with the increase in the initial dye concentration. This behavior is attributed to that the amount of dye adsorbed on the catalyst surface increases with the increase of dye concentration, but the intensity of light and irradiation time are constant, so the path length of photons entering the solution decreases and consequently the OH• radicals formed on the surface of ZnO decrease and thus results in the decrease of photodegradation efficiency [35].

3.3. Comparison of the photocatalytic activity of the synthesized and commercial ZnO

To evaluate the photocatalytic activity of the synthesized hexagonal cylinder-like bipods ZnO, the decolorization and TOC removal experiments using the synthesized ZnO and commercial ZnO as catalyst were carried out. As shown in Fig. 9, the decolorization efficiency of the dye by the synthesized ZnO is higher than that by the commercial ZnO after 45 min of reaction time. After 3 h of reaction time, the TOC removal efficiency of the dye by the synthesized ZnO and commercial ZnO is 65.3% and 49.8%, respectively. It is evident that the synthesized ZnO is more efficient for the mineralization and decomposition of the model compound as compared with the commercial ZnO powders. Similar results were reported earlier for the degradation of organic compound by ZnO photocatalyst with novel morphology. Sun et al. had synthesized dumbbell-shaped ZnO and found that 16–22% higher TOC removal efficiency was obtained by the dumbbell-shaped ZnO compared to commercial ZnO [36]. The good performance for the degradation of the dye by the synthesized ZnO may be attributed to its high specific surface area and excellent optical properties (as shown in Figs. 3 and 4).

3.4. Degradation pathway of Reactive Brilliant Red K-2BP

The samples of Reactive Brilliant Red K-2BP oxidized at different intervals were collected to determine the intermediate compounds by GC/MS and four compounds were detected (Isocyanatobenzene (D_1), Aniline (D_2), Phenol (D_3), Phthalic acid (D_4)). A tentative degradation pathway based on the GC/MS identification is proposed in Fig. 10. We theorize that the initial Reactive Brilliant Red K-2BP and the intermediates are degraded by direct oxidation, hydrolysis, and free radical attack. The C–N bonds are initially broken down to form compounds S_1, S_2, S_3 and S_4. Then the C–Cl, C–S bonds of compounds S_1 (oxidized by active radicals at the same time), S_2, S_3 and S_4 are cleaved to yield the corresponding

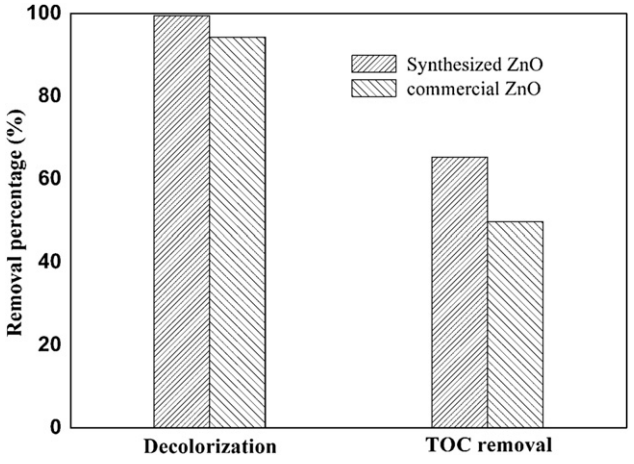

Fig. 9. Decolorization (after 45 min irradiation) and TOC removal (after 3 h irradiation) efficiencies of Reactive Brilliant Red K-2BP by the synthesized ZnO and commercial ZnO. Experimental conditions: [dye] = 50 mg/l, [ZnO] = 0.5 g/l and pH = 6.0.

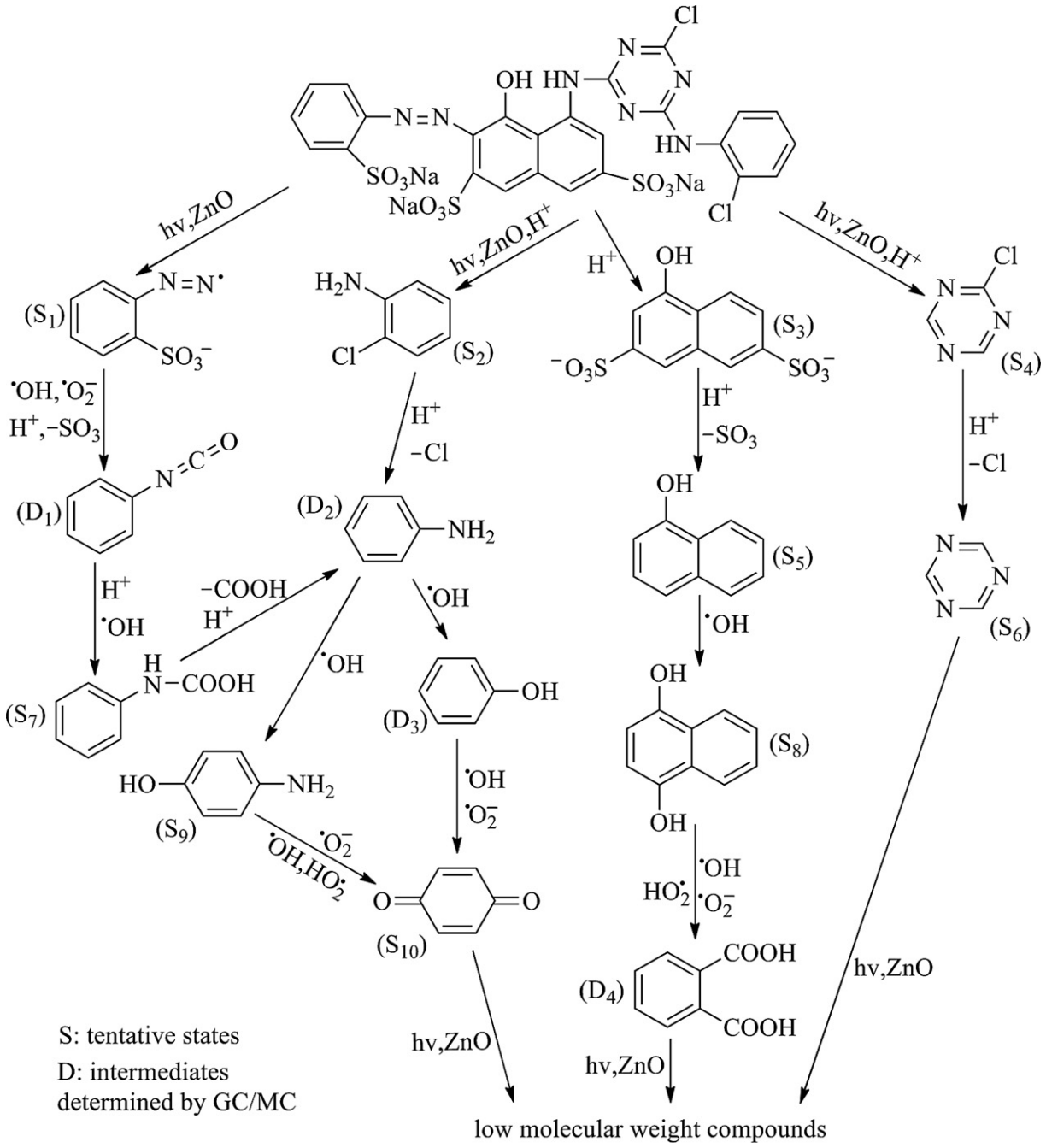

Fig. 10. Proposed pathways of the photocatalytic degradation of Reactive Brilliant Red K-2BP.

compounds D_1, D_2, S_5 and S_6. Compound D_1 can be hydrolyzed in aqueous solution to form S_7, which then could be decarboxylated to yield compound D_2. Compounds D_2 can be attacked by active radicals yielding S_9 and D_3, which could be further oxidized to yield compound S_{10}. Compound S_5 can be oxidized by active radicals yielding compound S_8 and generating D_4 by the breakdown of the aromatic ring. The compounds S_6, S_{10} and D_4 are further oxidized to yield low molecular weight compounds.

4. Conclusion

Single crystalline ZnO with hexagonal cylinder-like bipods morphologies have been successfully synthesized by a cationic surfactant-assisted hydrothermal microemulsion process. The characterization results show that the prepared ZnO microcrystal photocatalyst is pure and belongs to the hexagonal wurtzite family. The photocatalytic activity of the prepared ZnO has been evaluated by the degradation of Reactive Brilliant Red K-2BP in aqueous solution. Operational parameters such as ZnO dosage, pH value and dye concentration have significant influence on the photodegradation efficiency. For degradation of 50 mg/l of Reactive Brilliant Red K-2BP, the most suitable operation conditions are: catalyst dosage 0.5 g/l, pH value 6.0. Under the optimum conditions, the decolorization and TOC removal efficiencies are achieved 99.5% (45 min) and 69.3% (3 h), respectively, which is higher than that by the commercial ZnO. In addition, the possible degradation

pathways of the dye have been proposed. Overall, the good optical absorption properties of the as-prepared ZnO may be very interesting for further application on catalyst and chemical sensors.

Acknowledgments

The authors gratefully acknowledge the financial support from The Youth Fund of Henan Normal University (Grant No. 01036400069) and The National Natural Science Foundation of China (Grant No. 51174083).

References

[1] Jiang Y, Sun Y, Liu H, Zhu F, Yin H. Solar photocatalytic decolorization of C.I. basic blue 41 in an aqueous suspension of TiO_2–ZnO. Dyes and Pigments 2008;78:77–83.
[2] Neppolian B, Choi HC, Sakthivel S, Arabindoo B, Murugesan V. Solar light induced and TiO_2 assisted degradation of textile dye reactive blue 4. Chemosphere 2002;46:1173–81.
[3] Wang S, Li H. Kinetic modeling and mechanisms of dye adsorption on unburned carbon. Dyes and Pigments 2007;72:308–14.
[4] Farias J, Rossetti GH, Albizzati ED, Alfano OM. Solar degradation of formic acid: temperature effects on the photo–fenton reaction. Industrial and Engineering Chemistry Research 2007;46:7580–6.
[5] Pirkanniemi K, Sillanpaa M. Heterogeneous water phase catalysis as an environmental application: a review. Chemosphere 2002;48:1047–60.
[6] Curri ML, Comparelli R, Cozzoli PD, Mascolo G, Agostiano A. Colloidal oxide nanoparticles for the photocatalytic degradation of organic dye. Materials Science and Engineering C 2003;23:285–9.
[7] Yu JG, Yu XX. Hydrothermal synthesis and photocatalytic activity of zinc oxide hollow spheres. Environmental Science and Technology 2008;42:4902–7.
[8] Sakthivel S, Neppolian B, Shankar MV, Arabindoo B, Palanichamy M, Murugesan V. Solar photocatalytic degradation of azo dye: comparison of photocatalytic efficiency of ZnO and TiO_2. Solar Energy Materials and Solar Cells 2003;77:65–82.
[9] Huang MH, Wu Y, Feik H, Tran N, Weber E, Yang P. Catalytic growth of zinc oxide nanowires by vapor transport. Advanced Materials 2001;13:113–6.
[10] Si PC, Bian XF, Li H, Liu YX. Synthesis of ZnO nanowhiskers by a simple method. Materials Letters 2003;57:4079–82.
[11] Anas S, Mangalaraja RV, Ananthakumar S. Studies on the evolution of ZnO morphologies in a thermohydrolysis technique and evaluation of their functional properties. Journal of Hazardous Materials 2010;75:889–95.
[12] Peng ZW, Dai GZ, Chen P, Zhang QL, Wan Q, Zou BS. Synthesis, characterization and optical properties of star-like ZnO nanostructures. Materials Letters 2010;64:898–900.
[13] Wang FZ, Ye ZZ, Ma DW, Zhu LP, Zhuge F. Novel morphologies of ZnO nanotetrapods. Materials Letters 2005;59:560–3.
[14] Zhao JW, Qin LR, Xiao ZD, Zhang LD. Synthesis and characterization of novel flower-shaped ZnO nanostructures. Materials Chemistry and Physics 2007;105:194–8.
[15] Musić S, Šarić A, Popović S. Formation of nanosize ZnO particles by thermal decomposition of zinc acetylacetonate monohydrate. Ceramics International 2010;36:1117–23.
[16] Kim JH, Choi WC, Kim HY, Kang Y, Park YK. Preparation of mono-dispersed mixed metal oxide micro hollow spheres by homogeneous precipitation in a micro precipitator. Powder Technology 2005;153:166–75.
[17] Zhang ZQ, Mu J. Hydrothermal synthesis of ZnO nanobundles controlled by PEO-PPO-PEO block copolymers. Journal of Colloid and Interface Science 2007;307:79–82.
[18] Rani S, Suri P, Shishodia PK, Mehra RM. Synthesis of nanocrystalline ZnO powder via sol–gel route for dye-sensitized solar cells. Solar Energy Materials and Solar Cells 2008;92:1639–45.
[19] Komarneni S, Bruno M, Mariani E. Synthesis of ZnO with and without microwaves. Materials Research Bulletin 2000;35:1843–7.
[20] Sun GB, Cao MH, Wang YH, Hu CW, Liu YH, Ren L, et al. Anionic surfactant-assisted hydrothermal synthesis of high-aspect-ratio ZnO nanowires and their photoluminescence property. Materials Letters 2006;60:2777–82.
[21] Agrell J, Germani G, Järås SG, Boutonnet M. Production of hydrogen by partial oxidation of methanol over ZnO-supported palladium catalysts prepared by microemulsion technique. Applied Catalysis A 2003;242:233–45.
[22] Sun T, Qiu J. Novel morphologies of ZnO nanotetrapods. Materials Letters 2008;62:1528–31.
[23] Bitenc M, Dražić G, Orel ZC. Characterization of crystalline zinc oxide in the form of hexagonal bipods. Crystal Growth & Design 2010;10:830–7.
[24] Yang Z, Shi YY, Sun XL, Cao HT, Lu HM, Liu XD. The competition growth of ZnO microrods and nanorods in chemical bath deposition process. Materials Research Bulletin 2010;45:474–80.
[25] Liu YM, Lv H, Li SQ. Photocatalytic degradation of reactive brilliant blue KN-R by TiO_2/UV process. Desalination 2010;258:48–53.
[26] Wang BG, Shi EW, Zhong WZ. Twinning morphologies and mechanisms of ZnO crystallites under hydrothermal conditions. Crystal Research and Technology 1998;33:937–41.
[27] Jiang P, Zhou JJ, Fang HF, Wang CY, Wang Z, Xie SS. Hierarchical shelled ZnO structures made of bunched nanowire arrays. Advanced Functional Materials 2007;17:1303–10.
[28] Daud NK, Hameed BH. Decolorization of acid red 1 by fenton-like process using rice husk ash-based catalyst. Journal of Hazardous Materials 2010;176:938–44.
[29] Zhang GK, Lü F, Li M, Yang JL, Zhang XY, Huang BB. Synthesis of nanometer Bi_2WO_6 synthesized by sol–gel method and its visible-light photocatalytic activity for degradation of 4BS. Journal of Physics and Chemistry of Solids 2010;71:579–82.
[30] Ramirez JH, Maldonado-Hodar FJ, Perez-Cadenas AF, Moreno-Castilla C, Costa CA, Madeira LM. Azo-dye orange II degradation by heterogeneous fenton-like reaction using carbon–Fe catalysts. Applied Catalysis B 2007;75:312–23.
[31] Qamar M, Muneer M. A comparative photocatalytic activity of titanium dioxide and zinc oxide by investigating the degradation of vanillin. Desalination 2009;249:535–40.
[32] Brijesh P, Jonnalagadda SB, Tomar H, Singh P. ZnO assisted photocatalytic degradation of acridine orange in aqueous solution using visible irradiation. Desalination 2008;232:80–90.
[33] Ou HH, Lo SL, Wu CH. Exploring the interparticle electron transfer process in the photocatalytic oxidation of 4-chlorophenol. Journal of Hazardous Materials 2006;137:1362–70.
[34] Cao Y, Chen J, Huang L, Wang Y, Hou Y, Lu Y. Photocatalytic degradation of chlorfenapyr in aqueous suspension of TiO_2. Journal of Molecular Catalysis A 2005;233:61–6.
[35] Kansal SK, Singh M, Sud D. Studies on photodegradation of two commercial dyes in aqueous phase using different photocatalysts. Journal of Hazardous Materials 2007;141:581–90.
[36] Chen QQ, Wu PX, Li YY, Zhu NW, Dang Z. Heterogeneous photo-fenton photodegradation of reactive brilliant orange X-GN over iron-pillared montmorillonite under visible irradiation. Journal of Hazardous Materials 2009;168:901–8.